Zhou *et al. Stem Cell Research & Therapy* (2025) 16:233
https://doi.org/10.1186/s13287-025-04365-8

Stem Cell Research & Therapy

RESEARCH Open Access

Human umbilical cord mesenchymal stem cell-derived exosomes repair IBD by activating the SIRT1-FXR pathway in macrophages

Mengjiao Zhou[1,2], Bing Pei[3], Peipei Cai[1], Chengxue Yi[4], Francis Atim Akanyibah[1], Changkun Lyu[5] and Fei Mao[1,2*]

Abstract

Background Inflammatory bowel disease (IBD), a chronic immune disorder, has increasing global incidence and poor treatment outcome. Abnormal macrophage function is implicated in the pathophysiology of IBD. In this study, we investigated the mechanism by which human umbilical cord mesenchymal stem cell-derived exosomes (hucMSC-Ex) inhibit inflammation in IBD mouse and macrophage inflammation models.

Methods We established a dextran sodium sulfate (DSS)-induce BALB/c mice model of IBD and treated with hucMSC-Ex via tail vein to evaluate their repair effect on IBD mice. An in vitro macrophage inflammation model was established using lipopolysaccharide (LPS) and Nigericin (Nig) by stimulating mouse macrophage RAW264.7 and human myeloid leukemia mononuclear (THP-1) cells to assess the repair effect of hucMSC-Ex on macrophage inflammation. EX 527, an effective inhibitor of silent information regulator of transcription 1 (SIRT1), was employed in both the in vivo and in vitro models to explore the effect of hucMSC-Ex on the SIRT1-FXR (farnesoid X receptor) pathway in macrophages during the attenuation of inflammation.

Results HucMSC-Ex effectively inhibited inflammation in both the in vivo and in vitro models by up-regulating the expressions of SIRT1 and FXR, which reduced the acetylation level of FXR and inhibited the activation of NOD-like receptor thermal protein domain associated protein 3 (NLRP3) inflammasome. The addition of EX 527 further proved that hucMSC-Ex can reduce the acetylation of FXR by activating the SIRT1-FXR pathway, and the decrease of FXR acetylation was directly related to the inhibition of the activity of the NLRP3 inflammasome.

Conclusion HucMSC-Ex alleviates IBD by reducing the acetylation level of FXR through activating the SIRT1-FXR pathway in macrophages and directly negatively regulating the activation of NLRP3 inflammasomes, thus inhibiting the occurrence of the inflammatory process.

Keywords hucMSC-Ex, Macrophage, SIRT1-FXR pathway, NLRP3 inflammasome, IBD

[†]Mengjiao Zhou and Bing Pei contributed equally to this work.

*Correspondence:
Fei Mao
maofei2003@ujs.edu.cn
[1]Department of Laboratory Medicine, The Affiliated People's Hospital, Jiangsu University, No.8 Dianli Road, Zhenjiang, Jiangsu 212002, P. R. China
[2]Institute of Hematology, Jiangsu University, Zhenjiang, Jiangsu 212013, P. R. China
[3]Department of Clinical Laboratory, The Affiliated Suqian First People's Hospital of Nanjing Medical University, Suqian, Jiangsu 223800, P. R. China
[4]School of Medical Technology, Zhenjiang College, Zhenjiang, Jiangsu 212028, P. R. China
[5]School of Medical Technology, Shangqiu Medical College Shangqiu, Shangqiu, Henan 476100, P. R. China

Introduction

IBD, which includes Crohn's disease (CD) and ulcerative colitis (UC), is a complex disease whose pathogenesis involves genetic factors, immune disorders, and intestinal microbiota changes [1]. IBD has evolved into a global disease with increasing prevalence and a serious impact on patient's quality of life [2]. IBD is also a major risk factor for gastrointestinal tumors, including colon cancer, small intestinal adenocarcinoma, intestinal lymphoma, and anal canal cancer. Therefore, IBD intervention can prevent the occurrence of gastrointestinal tumors [3].At present, a variety of regimens are used in the treatment of IBD, such as immunomodulators, thiopurine drugs and monoclonal antibodies [4], but the treatment effect is still not ideal. Therefore, it is urgent to find beneficial treatment methods that can adapt to the complex composition and microbial environment of the gut.

Mesenchymal stem cells (MSCs), as a kind of non-hematopoietic pluripotent stem cells, have the ability to self-renew and differentiate into mesoderm tissues, such as lipoblasts and osteoblasts, and can exert immune regulation function through intercellular contact or paracrine pathway [5]. Exosomes originate from vesicles formed in the intracellular multivesicular body (MVB) and released into the cell through the combination of multivesicular and plasma membranes. The diameter of exosomes is about 30–200 nm, and they are cup-shaped under an electron microscope, with good biological characteristics such as compatibility, stability, and low toxicity. Exosomes are found in almost all body fluids, such as blood, breast milk, cerebrospinal fluid, and amniotic fluid [6, 7]. Many studies have reported that exosomes can alleviate IBD through various mechanisms. Macrophage-derived exosomes inhibited intestinal barrier dysfunction caused by transmembrane and immunoglobulin domain containing 1 (TMIGD1) by releasing miR-223 [8], exosomes derived from human-adipose derived stem cells (hADSCs) can reshape the cell structure in the colonic mucosa of IBD mice and promote the growth of colonic organoids, which enables it to counteract the inflammatory response induced by tumor necrosis factor-α (TNF-α) [9].

FXR, as a key receptor for bile acid regulation, is mainly expressed in hepato-intestinal tissues [10]. Studies have shown that SIRT1 can directly act on FXR, causing it to deacetylate and change its activity. The K217 in the hinge region of FXR is the main acetylation site, and the acetylation level of FXR is increased in mouse models with metabolic disorders [11]. At present, the SIRT1-FXR pathway is mainly studied in liver diseases. For example, Celastrol can improve cholestasis and restore bile acid metabolic homeostasis to alleviate liver inflammation by activating the SIRT1-FXR signaling pathway [12]. The activation of the SIRT1-FXR signaling pathway also mitigates triptolide-induced hepatotoxicity in rats [13].

FXR also expressed in innate immune cells such as macrophages, natural killer cells and dendritic cells. In normal physiology and disease, innate immune cells are involved in communication between tissues, and activation of FXR can alleviate immune dysfunction caused by inflammation in various liver and intestinal disease models [14]. Among them, we focus on the role of FXR in macrophages, which are specialized immune cells that engulf and eliminate foreign organisms as well as apoptotic cells. M1-type macrophages release pro-inflammatory cytokines, making it difficult for damaged wounds to heal, while M2-type macrophages promote tissue repair by secreting anti-inflammatory cytokines. The imbalance between the two activities will lead to persistent inflammation, hinder the normal repair process, and lead to various diseases [15]. The gastrointestinal tract houses the largest total number of macrophages, and intestinal macrophages play a key role in chronic intestinal inflammation following damage to the intestinal barrier. The destruction of intestinal ecological environment can easily trigger the activation of lamina propria macrophages in the intestine by bacterial products, resulting in chronic inflammation [16]. As an important component of the innate immune system, macrophages play an important role in regulating intestinal homeostasis and inflammatory response [17]. The dysfunction of intestinal inflammation resolution in patients with IBD is closely related to macrophages, making macrophages potential therapeutic targets for IBD [18].When macrophages perceive inflammatory stimuli, they regulate their own metabolic signals, including the activation of the NLRP3 inflammasome [19]. Macrophages are the main source of monocyte chemotactic protein-1 (MCP-1), which can promote the infiltration and migration of macrophages to the place where the inflammatory reaction occurs. Chenodeoxycholic acid (CDCA) can inhibit the expression of MCP-1, and the specific mechanism is that CDCA promotes FXR to bind to a DR4 element in the promoter region of MCP-1, thereby inhibiting the expression of MCP-1 [20]. Some scholars have found that the use of FXR activator GW4064 can alleviate LPS-induced liver injury in mouse nonalcoholic fatty liver disease (NAFLD) models, reduce macrophage infiltration, and inhibit the release of macrophage inflammatory factors [21]. Therefore, regulating the expression of FXR to affect the functional changes of macrophages is of great significance for the treatment of diseases.

The pleiotropic effect of FXR is necessary for intestinal health, and FXR plays an important role in IBD as a key receptor regulating bile acid synthesis, as well as inhibiting inflammation and tumorigenesis [22].

However, whether the changes in the acetylation level of FXR in the gut and SIRT1-FXR pathway are related to the pathogenesis of IBD has not been widely studied. Studies have shown that FXR directly negatively regulates the activation of NLRP3 inflammasomes in macrophages, which can improve bile acid metabolism and thus alleviate liver diseases [23]. However, it is unknown whether the changes in FXR acetylation level are related to the activity of NLRP3 inflammasome in macrophages. Therefore, this study explored the mechanism of hucMSC-Ex repair of IBD, and whether hucMSC-Ex directly negatively regulates the activation of NLRP3 inflammasome by modulating FXR acetylation level in macrophages. This provides a new mechanistic proof on the mitigation effect of hucMSC-Ex in IBD.

Materials and methods

Cell culture

Human umbilical cord mesenchymal stem cells were isolated and cultured from fresh human umbilical cord of healthy mothers (with the informed consent of the mothers and their families) and cultured with α-MEM culture medium. RAW264.7 and THP-1 cells were purchased from Procell company (Wuhan, China), and treated with 10% fetal bovine serum (FBS; Zhejiang Tianhang Biotechnology Co.,Ltd., China). RAW264.7 cells were cultured in DMEM medium (Hyclone, USA) containing 10% FBS and THP-1cells were cultured in 1640 medium (Hyclone, USA) containing 10% FBS. Cells were cultured in the 5% CO_2 incubator at 37℃.

Extraction of hucMSC-Ex

The supernatant stored at -80℃ was thawed at -20℃ first, and then 4℃. The supernatant was centrifuged at 4℃, 2000 g, for 30minafter the ice was completely dissolved to remove cell debris; the supernatant collected after centrifugation was further centrifuged at 4℃, 10,000 g, for 30 min to remove subcellular debris. The supernatant collected after centrifugation was placed in a 100KD ultrafiltration centrifuge tube and centrifuged at 4℃, 2000 g. After the ultrafiltrate was collected, it was centrifuged at 4℃, 100,000 g, for 2 h, the supernatant was removed, the phosphate buffered saline (PBS) was added for cleaning and full suspension, and further centrifuged at 4℃, 100,000 g, for 2 h. The final supernatant was obtained. According to the amount of exosome precipitates, an appropriate amount of PBS was added to completely dissolved the precipitate in PBS, followed by removing the supernatant. The exosomes were filtered with an aseptic filter and divided into aseptic EP tubes (Axygen, USA). Few exosomes were taken for identification, and the rest were stored at -80℃ for later use.

Transmission electron microscope (TEM) scanning analysis

The freshly extracted hucMSC-Ex was diluted with PBS, the diluted drops of hucMSC-Ex were added to the copper mesh, and after standing at room temperature for 2–3 min, the surrounding excess liquid was absorbed with clean filter paper, and then re-stained with 3% phosphotungstic acid for 1–2 min. The relevant field of view was photographed with transmission electron microscope after natural drying.

Nanosight nanoparticle tracking analysis (NTA)

1μL of freshly extracted hucMSC-Ex was thoroughly mixed with pure water by the dilution ratio of 1:2000, after standard liquid was used to calibrate and clean the pipe of instrument until there was no residual particle number, the hucMSC-Ex diluted liquid after mixing was absorbed with 1mL sterile syringe and slowly pushed into the instrument pipe system for the detection and analysis of hucMSC-Ex particle number and particle size.

Western blot analysis

RIPA lysate (Solarbio, Beijing, China) was applied to mouse colon tissues and cells, and the protein concentration was analyzed by the BCA method. The proteins were isolated on 12% sodium dodecyl sulfate-polyacrylamide gel electrophoresis (SDS-PAGE), then transferred to a PVDF membrane (Millipore, Billerica, MA, USA) and sealed with 5% skim milk to reduce exposure to nonspecific antigens. PVDF membrane was incubated with primary antibodies: CD9 antibody (1:500; Affinity Biosciences, OH, USA), CD81 antibody (1:500; Affinity Biosciences, OH, USA), HSP70 antibody (1:500; Affinity Biosciences, OH, USA), Calnexin antibody (1:500; Affinity Biosciences, OH, USA), SIRT1 antibody (1:1000; Proteintech Group, USA), FXR antibody (1:600; Proteintech Group, USA), NLRP3 antibody (1:1000; Proteintech Group, USA), Caspase 1 antibody (1:1000; Proteintech Group, USA), Caspase 1 p20 antibody (1:700; Affinity Biosciences, OH, USA) and IL-1β antibody (1:1000; Affinity Bioscience, OH, USA) at 4℃ overnight. The primary antibody was removed the next day, and then the secondary antibody bound with horseradish peroxidase was incubated at 37℃ for 1 h at room temperature. Finally, the chemical gel imaging system (GE Healthcare Life Sciences China, Beijing, China) was employed to observe the protein bands.

Animals

Male BALB/c mice (age: 6-8weeks, weight: 20 ± 3 g) were purchased from the Animal Center of Jiangsu University (Zhenjiang, China). Animal experiments performed were approved by the Ethics Committee and the Experimental Animal Management and Use Committee of Jiangsu University. All mice were killed on the tenth day of the

experiment. The mice were euthanized not by anesthetic injection, but by physical means of cervical dislocation. The work in this study has been reported in line with the ARRIVE guidelines 2.0.

Clinical colon tissue samples

Clinical colon tissue samples were collected from IBD patients ($n = 10$) and healthy individuals ($n = 10$) who visited Nanjing Jiangning Hospital from June 2022 to June 2023. Patients with IBD have no other diseases other than IBD. The colon specimens of the healthy control group refer to those who came to the pathology department of the hospital for colon pathological section, but were not diagnosed with IBD and had no obvious gastrointestinal inflammation. The collection of specimens was approved by the ethics committee of the hospital and with the consent of the patient and his or her family, then the clinical colon tissues were made into paraffin sections.

Construction of animal IBD model

The mice were randomly divided into 3 groups ($n = 6$/group): negative control group (NC group), DSS-induced colitis group (IBD group), and hucMSC-Ex treatment of colitis group (hucMSC-Ex group). Mice in the NC group drank autoclaved water, while mice in the DSS and the hucMSC-Ex groups drank 3%DSS (MP Biomedicals, CA, USA) dissolved in autoclaved water every day. On the third, sixth and ninth day, every mouse in the hucMSC-Ex group was injected with 1 mg hucMSC-Ex by the tail vein, and mice in the DSS group were injected with an equal volume of PBS. Body weight, fecal traits, and activity status of mice were recorded at the same time every day, and disease activity index (DAI) was analyzed. All mice were killed on the 10th day, and the spleen and colon of mice were harvested on the same day. The gross view of the colon and spleen of mice was observed and photographed, and the tissues were immersed in PBS pre-cooled at 4℃. Some mice colon and spleen tissues were fixed in 4% paraformaldehyde for preparation of paraffin sections, and the remaining colon tissues were used for follow-up experiments.

Treatment of animal models with EX527

Using SIRT1 inhibitor EX 527 (Selleck, USA), the mice were divided into five groups: NC group, DSS group, hucMSC-Ex group, DSS + EX 527 group, and hucMSC-Ex + EX 527 group, with 6 mice in each group. The NC group drank autoclaved water and the remaining groups were given 3% DSS to induce IBD. Mice in the hucMSC-Ex and hucMSC-Ex + EX 527 groups were injected with 1 mg of hucMSC-Ex each mouse through the tail vein on the third, sixth, and ninth days after drinking the 3% DSS. Mice in the DSS + EX 527 and hucMSC-Ex + EX 527 groups were subjected to intraperitoneal injection of EX 527 every day at a dosage of 10 mg/kg with a dosage volume of 300μL each. The weight, fecal traits, and living status of mice were recorded at a fixed time every day, and the mice were killed at when obvious adverse conditions occurred. The spleen and colon of mice were isolated on the same day, and excess components such as mesentery and fat were removed. The gross view of colon and spleen of mice were observed and photographed, and the tissues were immersed in PBS pre-cooled at 4℃. Some of the colon and spleen tissues were fixed in 4% paraformaldehyde for preparation of paraffin sections, and the remaining colon tissues were used for other experiments.

Construction of macrophage inflammation models

RAW264.7 cells were centrifugally suspended and then spread on a six-well plate according to the number of 1×10^6/ well, and shaken to obtain a uniformity, followed by placing them in a cell incubator for culture (37℃, 5% CO_2), when the cells grew to a density of 60-80%, LPS (Sigma, USA) and Nig (Selleck, USA) were used to stimulate the inflammatory response. In the experiment, RAW264.7 cells were divided into three groups: NC group, LPS + Nig group, and hucMSC-Ex + Nig group. The LPS + Nig and hucMSC-Ex + Nig groups were incubated with 1 μg/mL LPS, while the hucMSC-Ex + Nig group was incubated with 200 μg/mL hucMSC-Ex. After 4 h of culture in the cell incubator, 1μM of Nig was added to the LPS + Nig and hucMSC-Ex + Nig groups. After a total culture time of 6 hours, cell RNA was extracted, and cell protein was extracted after 12 h of culture.

THP-1 is a kind of suspended cell, to differentiate cells into macrophages, they were induced with 50ng/mL Phorbol 12-Myristate 13-Acetate (PMA; Sigma, USA). The THP-1 cells were spread on a six-well plate according to the density of 2×10^6/well, adding PMA, and cells were cultured in the cell incubator for 16 h before replacing with the new cell culture medium. Follow-up operations are the same as those of RAW264.7. After 2 h of incubation, 1μM of Nig was added to the LPS + Nig and hucMSC-Ex + Nig groups and further incubated. After a total culture time of 3 h, cell RNA was extracted, and cell protein was extracted after 6 hours.

Treatment of macrophage inflammation models with EX527

RAW264.7 cells were divided into five groups: NC group, LPS + Nig group, hucMSC-Ex + Nig group, LPS + EX527 + Nig group, and hucMSC-Ex + EX 527 + Nig group. The LPS + Nig, hucMSC-Ex + Nig, LPS + EX 527 + Nig, and hucMSC-Ex + EX 527 + Nig groups were treated with 1 μg/mL LPS. The hucMSC-Ex + Nig and hucMSC-Ex + EX 527 + Nig groups were treated with 200 μg/mL of hucMSC-Ex, while the LPS + EX 527 + Nig

Table 1 Sequences of primers

Species	Gene	Sequences
Mouse	β-actin-F	GTGCTATGTTGCTCTAGACTTCG
	β-actin-R	ATGCCACAGGATTCCATACC
	IL-10-F	TTCTTTCAAACAAAGGACCAGC
	IL-10-R	GCAACCCAAGTAACCCTTAAAG
	IL-6-F	CTCCCAACAGACCTGTCTATAC
	IL-6-R	CCATTGCACAACTCTTTTCTCA
	TNF-α-F	ATGTCTCAGCCTCTTCTCATTC
	TNF-α-R	GCTTGTCACTCGAATTTTGAGA
	IL-1β-F	CACTACAGGCTCCGAGATGAACAAC
	IL-1β-R	TGTCGTTGCTTGGTTCTCCTTGTAC
	SIRT1-F	CGCTGTGGCAGATTGTTATTAA
	SIRT1-R	TTGATCTGAAGTCAGGAATCCC
	FXR-F	GCCACAGATTTCCTCCTCGT
	FXR-R	TCCCTGGTACCCAGTCTCAG
	NLRP3-F	GCTGCGATCAACAGGCGAGAC
	NLRP3-R	CCATCCACTCTTCTTCAAGGCTGTC
	Caspase 1-F	GAGGGATTTCTTAACGGATGCA
	Caspase 1-R	TCACAAGACCAGGCATATTCTT

Table 2 Sequences of primers

Species	Gene	Sequences
Human	β-actin-F	CCTGGCACCCAGCACAAT
	β-actin-R	GGGCCGGACTCGTCATAC
	IL-10-F	GTTGTTAAAGGAGTCCTTGCTG
	IL-10-R	TTCACAGGGAAGAAATCGATGA
	IL-6-F	CACTGGTCTTTTGGAGTTTGAG
	IL-6-R	GGACTTTTGTACTCATCTGCAC
	TNF-α-F	AAGGACACCATGAGCACTGAAAGC
	TNF-α-R	AGGAAGGAGAAGAGGCTGAGGAAC
	IL-1β-F	GCCAGTGAAATGATGGCTTATT
	IL-1β-R	AGGAGCACTTCATCTGTTTAGG
	SIRT1-F	TATACCCAGAACATAGACACGC
	SIRT1-R	CTCTGGTTTCATGATAGCAAGC
	FXR-F	CAACAAAGTCATGCAGGGAGAA
	FXR-R	TGATTGGTTGCCATTTCCGTC
	NLRP3-F	CTTGCCGACGATGCCTTCCTG
	NLRP3-R	GCTGTCATTGTCCTGGTGTCTTCC
	Caspase 1-F	GAAGAAACACTCTGAGCAAGTC
	Caspase 1-R	GATGATGATCACCTTCGGTTTG

and hucMSC-Ex + EX 527 + Nig groups were treated with 10μM EX 527. After 4 h of culture, the LPS + Nig, hucMSC-Ex + Nig, LPS + EX 527 + Nig, and hucMSC-Ex + EX 527 + Nig groups were treated with 1μM of Nig, and the RNA and protein were extracted after a total culture time of 6 h and 12 h respectively.

The treatment of THP-1 was similar to RAW264.7 cells. After 2 h of culture and incubation, the LPS + Nig, hucMSC-Ex + Nig, LPS + EX 527 + Nig, and hucMSC-Ex + EX 527 + Nig groups were treated with 1μM of Nig. After a total culture time of 3 h, the RNA was extracted, and after 6 h, cell protein was extracted.

Real-time fluorescence quantitative PCR

Trizol (Vazyme, Nanjing, China) was added to tissues or cells, followed by chloroform, and RNA was extracted at 4℃. The cDNA was obtained by the corresponding reverse transcription kit (Vazyme, Nanjing, China), and real-time fluorescent quantitative PCR (qRT-PCR) was performed in the Step One Plus real-time PCR system (ABI) to detect the expression of the target gene. The sequences of primers used are shown in Tables 1 and 2.

Immunohistochemical (IHC) analysis

The tissue sections were dried in an oven at 56℃ (for at least 6 hours), dewaxed with xylene and gradient concentration of ethanol, and endogenous peroxidase was blocked with 3% hydrogen peroxide solution. This was followed by heat-repair of antigen with freshly configured 0.01 M citrate buffer, then were closed at room temperature with 5% BSA for 30 minutes. The sections were incubated with SIRT1 antibody (1:200, Proteintech Group, USA), FXR antibody (1:200, Proteintech Group, USA), and NLRP3 antibody (1:200, Proteintech Group, USA) overnight, followed by the secondary antibodies at 37℃ for 30 minutes. The SABC was incubated at 37℃ for 30 minutes, 3,3'-diaminobenzidin (DAB) and hematoxylin were applied, and the impurities were rinsed under running water for 30 min, followed by dehydration, sealing, natural drying, and microscopic analysis.

Hematoxylin and Eosin (H&E) staining

Some of the mice colon and spleen tissues were fixed in 4% paraformaldehyde, embedded in paraffin, and sliced with a microtome. The sections were fixed on a slide, dewaxed, stained with H&E, and finally scanned and analyzed with a pathological biopsy scanner.

Immunofluorescence (IF)

The cells in the culture plate were cleaned with PBS, fixed with 4% paraformaldehyde at room temperature for 20 min, then the cell membrane was broken by 0.1% TritonX-100 and closed with 5% BSA at room temperature for 30 min. Caspase 1 antibody (1:300, Proteintech Group, USA) was added for overnight incubation at 4℃. On the second day, the primary antibody was discarded and added to the fluorescent secondary antibody, cells were incubated at room temperature for 1 h, the nucleus was stained with 4 ', 6-diaminidine-2-phenylindoline dihydrochloride (DAPI), and the outcome was photographed and analyzed with the super-resolution microscope in time.

Immunoprecipitation (IP)

To analyze the effect of changes in inflammatory response on the acetylation level of FXR, agarose

beads were connected with FXR antibodies, FXR was enriched by agarose beads, and then the acetylation molecule acetylated-lysine (Ac-Lys) was detected by FXR antibodies. Mouse colonic mucosa or cell suspension was lysed with an ultrasonic breaker. The lysate was mixed with FXR antibody (Cell Signaling Technology, USA), and G-agarose beads (Beyotime Biotechnology, China) were added overnight at 4℃. The suspension was washed about 5 times with IP lysis buffer, followed by a Western blot assay of FXR and Ac-Lys (Cell Signaling Technology, USA) using corresponding antibodies.

Statistical analysis

The GraphPad Primer 9 software was used for statistical significance analysis and mapping of the data. T-test or one-way ANOVA was used to analyze whether there were statistical differences between the data in each group. * indicates $P<0.05$, ** indicates $P<0.01$, and *** indicates $P<0.001$. (Data expressed as $\overline{X} \pm \mathrm{SD}$).

Results

Identification of hucMSC-Ex

Transmission electron microscopy showed that the extract was cup-shaped and had a complete vesicle structure, which was constituent with the hucMSC-Ex morphological structure (Fig. 1A). The result of NTA indicated that the number of particles extracted was 3.2×10^{11} and the particle size of exosomes was 189.2 nm (Fig. 1B). Western blot results showed that hucMSC-Ex expressed CD9, CD81, and heat shock protein 70 (HSP70), but did not express Calnexin, which met the criteria for identification of exosome surface markers (Fig. 1C). The above results shows that the substance extracted is hucMSC-Ex and meets the requirements of exosome identification.

hucMSC-Ex repairs DSS-induced mouse model of IBD

Mice fed 3% DSS were used to construct the IBD model, and 1 mg hucMSC-Ex was injected through the tail vein to repair the IBD. The results showed that the weight of mice in the NC group increased steadily every day, the DSS group began to decrease sharply on the sixth day, while the hucMSC-Ex group had a moderate weight loss compared to the DSS group (Fig. 2A). DAI score showed that the DSS and hucMSC-Ex groups experienced bloody and loose stools from the third day, but while the DSS group showed an increasingly severity after the third day, the hucMSC-Ex group rather improved from the sixth day, where the DAI score began to slowly decline (Fig. 2B). The gross view of the colon of the mice showed that the colon length of the mice in the DSS group was shorter, while that of the hucMSC-Ex group had recovered significantly (Fig. 2C). Moreover, the spleen of the DSS group was enlarged, while that of the hucMSC-Ex group had reduced splenomegaly (Fig. 2D). H&E staining of the colon and spleen showed that the colon tissue structure of the DSS group was significantly disordered and the normal glandular structure was destroyed, while the hucMSC-Ex group had a more complete and clearer tissue structure. Under DSS, the epithelial cells of the colon were severely damaged, the crypt structure disappeared and the inflammatory cell infiltration increased. But hucMSC-Ex can stall that process (Fig. 2E). Spleen nodules of mice in the DSS group were significantly damaged, while those in the hucMSC-Ex group were significantly restored (Fig. 2F). Inflammatory factors in the colon tissues were analyzed by qRT-PCR and the results showed that the mRNA expression levels of pro-inflammatory factors TNF-α and IL-6 in the DSS group were higher than those in the hucMSC-Ex group, while the anti-inflammatory factor IL-10 was lower than in the hucMSC-Ex group (Fig. 2G). These observations indicate

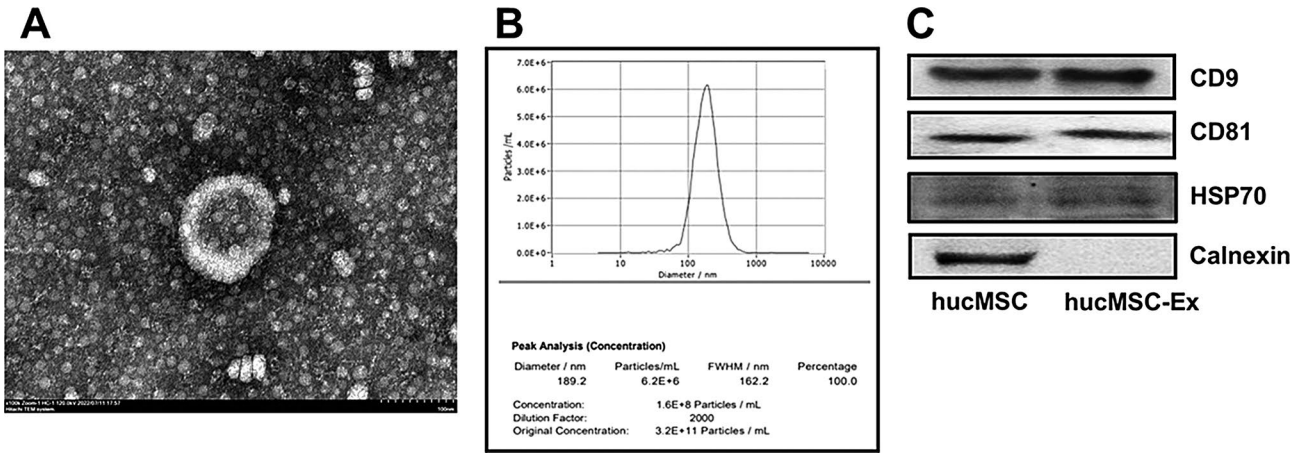

Fig. 1 Identification of hucMSC-Ex. **(A)** Morphology of hucMSC-Ex under transmission electron microscopy (scale bar = 100 nm); **(B)** Identification of the particle size and number of hucMSC-Ex by using the nanoparticle tracking analyzer; **(C)** The surface markers of hucMSC and hucMSC-Ex were detected by Western blot

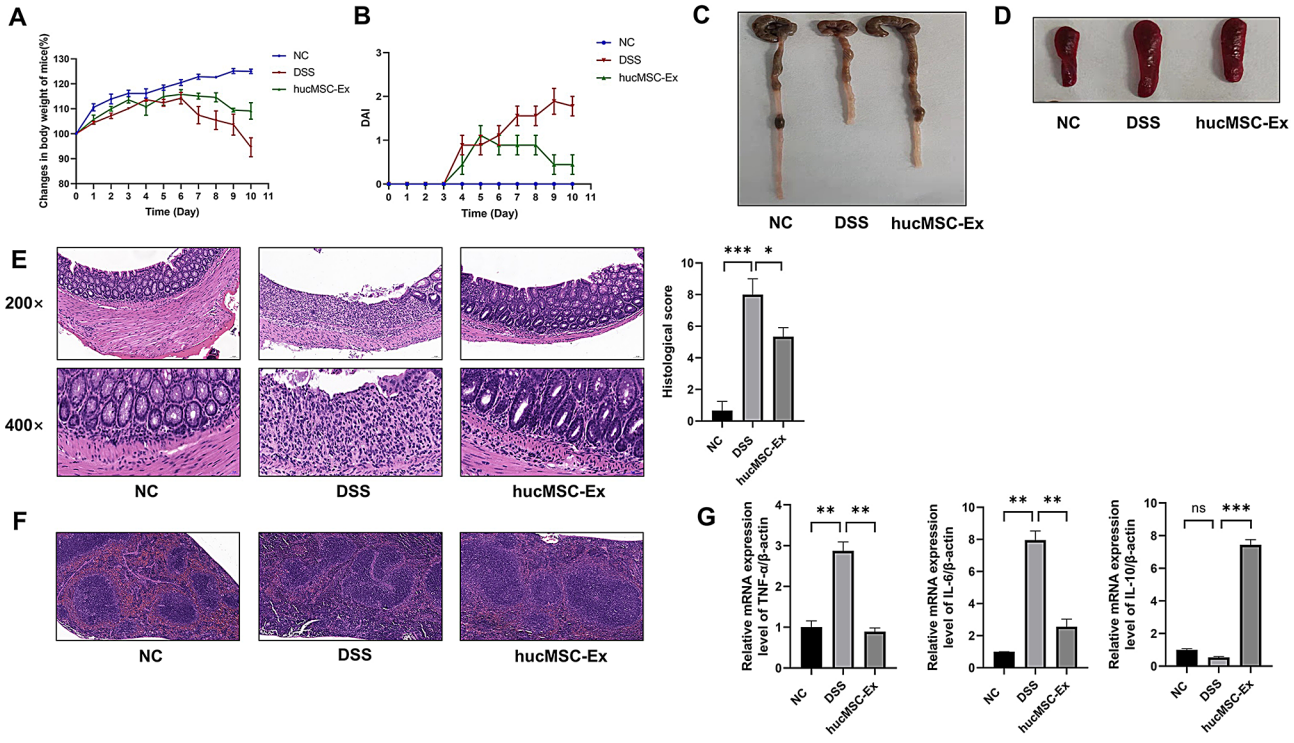

Fig. 2 hucMSC-Ex repairs DSS-induced IBD in mice. **(A)** Percentage of weight loss in mice ($n = 3$ independent experiments); **(B)** Assessment of DAI in mice ($n = 3$ independent experiments); **(C)** Gross view of the colons of mice; **(D)** Gross view of the spleens of mice; **(E)** H&E staining of the colon tissues of mice (200×, scale bar = 50 μm; 400×, scale bar = 20 μm) and the histological score of the colons of mice; **(F)** H&E staining of the spleen tissues of mice (200×, scale bar = 50 μm); **(G)**The mRNA expression levels of inflammatory factors (TNF-α, IL-6, and IL-10) in colon tissues of mice by qRT-PCR ($n = 3$ independent experiments). $^{*}P < 0.05$, $^{**}P < 0.01$, $^{***}P < 0.001$

that hucMSC-Ex alleviates DSS-induced IBD in mice by ameliorating the symptoms and repairing tissue damage.

Differences in FXR and Ac-Lys expression in the colons of healthy people and IBD patients

The expression of FXR and Ac-Lys in the colon tissues of healthy people and IBD patients was analyzed by IF and IHC. It was found that the expression of Ac-Lys in the colon tissues of healthy people was lower than that of IBD patients, while FXR was higher in healthy individuals than IBD patients by IF test (Fig. 3A). Meanwhile, the same conclusion was obtained by the IHC experiments (Fig. 3B).

hucMSC-Ex activates SIRT1 and FXR while inhibits FXR acetylation and NLRP3 inflammasomes in mice colons

Western blot analysis of the expression levels of SIRT1, FXR, and NLRP3 inflammasome-related markers (NLRP3, Caspase 1, Caspase 1 p20, and IL-1β) in mice colon tissues showed that protein expression levels of SIRT1 and FXR decreased in the DSS group but increased after hucMSC-Ex treatment. The expression of NLRP3 inflammasome-related molecules (NLRP3, Caspase 1, Caspase 1 p20, and IL-1β) was increased in the DSS group but decreased in the hucMSC-Ex group (Fig. 4A). Moreover, qRT-PCR showed that the mRNA expression levels of SIRT1 and FXR in the colon tissues of mice in the DSS group decreased, while NLRP3 inflammasome-related molecules increased, and the influence of DSS was reversed under hucMSC-Ex (Fig. 4B). In addition, IP test showed that the level of FXR acetylation in the colon tissues of the DSS group was higher than that of the hucMSC-Ex group (Fig. 4C). IHC was used to further confirm these observations, revealing that SIRT1 and FXR in the DSS group were decreased, and NLRP3 was increased. However, hucMSC-Ex increased SIRT1 and FXR, and reduced NLRP3 (Fig. 4D).

hucMSC-Ex activates SIRT1 and FXR while inhibits FXR acetylation and NLRP3 inflammasomes in macrophages

LPS was used to induce the macrophage inflammation model and Nigericin employed to activate the NLRP3 inflammasome in macrophages. The mRNA expression levels of inflammatory factors (TNF-α, IL-6, and IL-10) in RAW264.7 and THP-1 were analyzed by qRT-PCR. It was revealed that the mRNA expression levels of pro-inflammatory factors TNF-α and IL-6 in the LPS + Nig group were higher than the hucMSC-Ex + Nig group. Conversely, the expression level of the anti-inflammatory factor IL-10 was lower in the LPS + Nig group than the

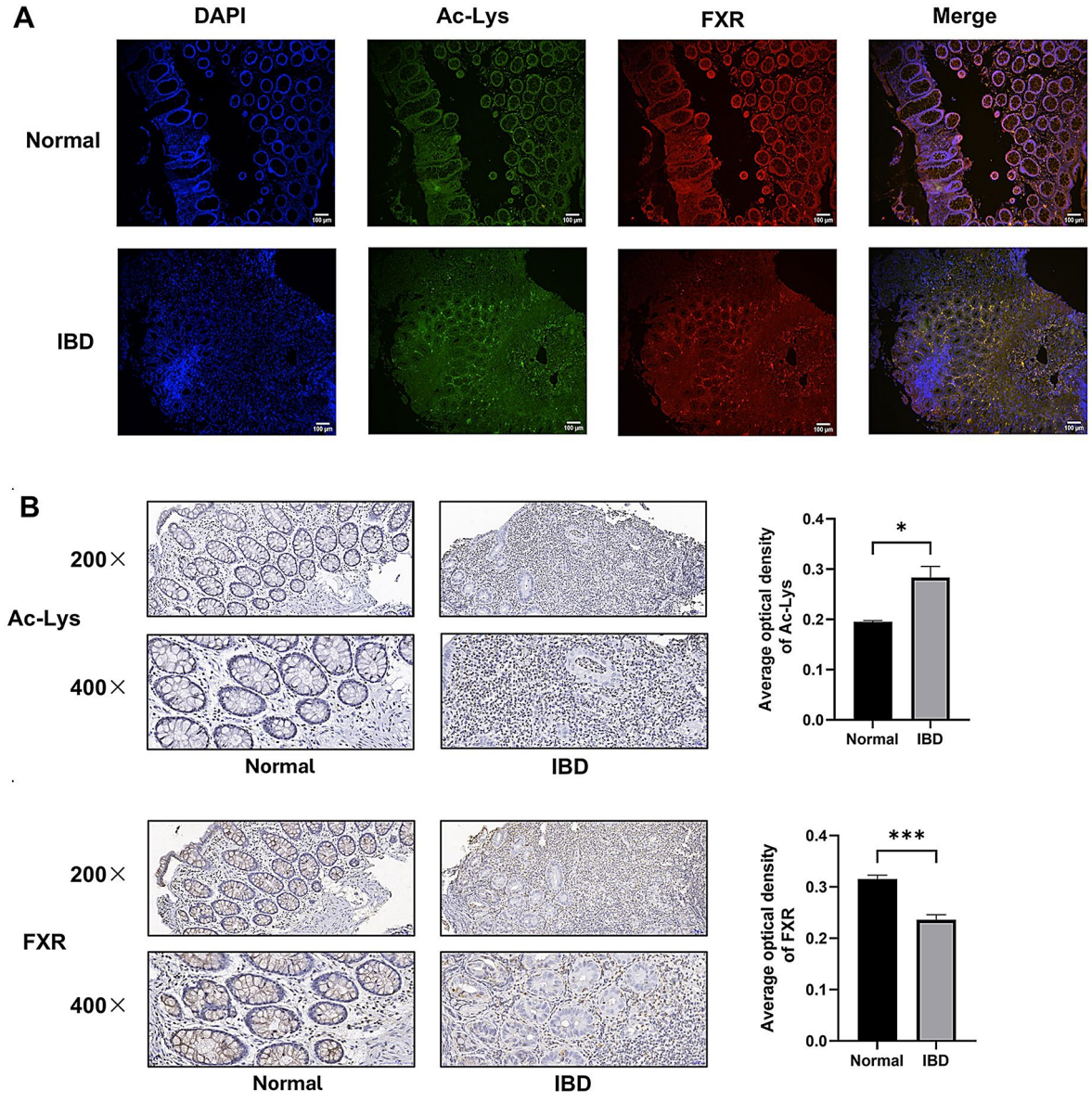

Fig. 3 Differences in FXR and Ac-Lys expression in the colons of healthy people and IBD patients. **(A)** The expression of Ac-Lys and FXR by IF in colon tissues of healthy people and IBD patients (100×, scale bar = 100 μm); (**B)** Location of Ac-Lys and FXR by IHC detection in colon tissues of healthy people and IBD patients (200×, scale bar = 50 μm; 400×, scale bar = 20 μm) and the relevant average optical density analysis ($n = 3$ independent experiments)

hucMSC-Ex + Nig group (Fig. 5A). Western blot analysis of SIRT1, FXR, and NLRP3 inflammasome-related molecules in RAW264.7 and THP-1 showed that SIRT1 and FXR were decreased in the LPS + Nig group but increased in the hucMSC-Ex + Nig group, and NLRP3 inflammasome-related molecules were increased in the LPS + Nig group but decreased in the hucMSC-Ex + Nig group (Fig. 5B). qRT-PCR results showed a similar trend of decreased SIRT1 and FXR mRNA expression in LPS + Nig group but increased expression in the hucMSC-Ex + Nig group. The mRNA expression of NLRP3 inflammasome-related molecules was also elevated in the LPS + Nig group (Fig. 5C). IP test results showed higher acetylation of FXR in LPS + Nig group of RAW264.7 compared to the hucMSC-Ex + Nig group (Fig. 5D). In addition, IF revealed that Caspase 1 expression in RAW264.7 of the LPS + Nig group was higher compared to the hucMSC-Ex + Nig group (Fig. 5E).

hucMSC-Ex mitigates the effects of SIRT1 inhibitor EX 527 on IBD mice models

We found that after intraperitoneal injection of the SIRT1 inhibitor, EX 527, the inflammatory response in mice in the DSS + EX 527 group was more obvious than that in the DSS group, while the effect of EX 527 was significantly alleviated in the hucMSC-Ex + EX 527 group.

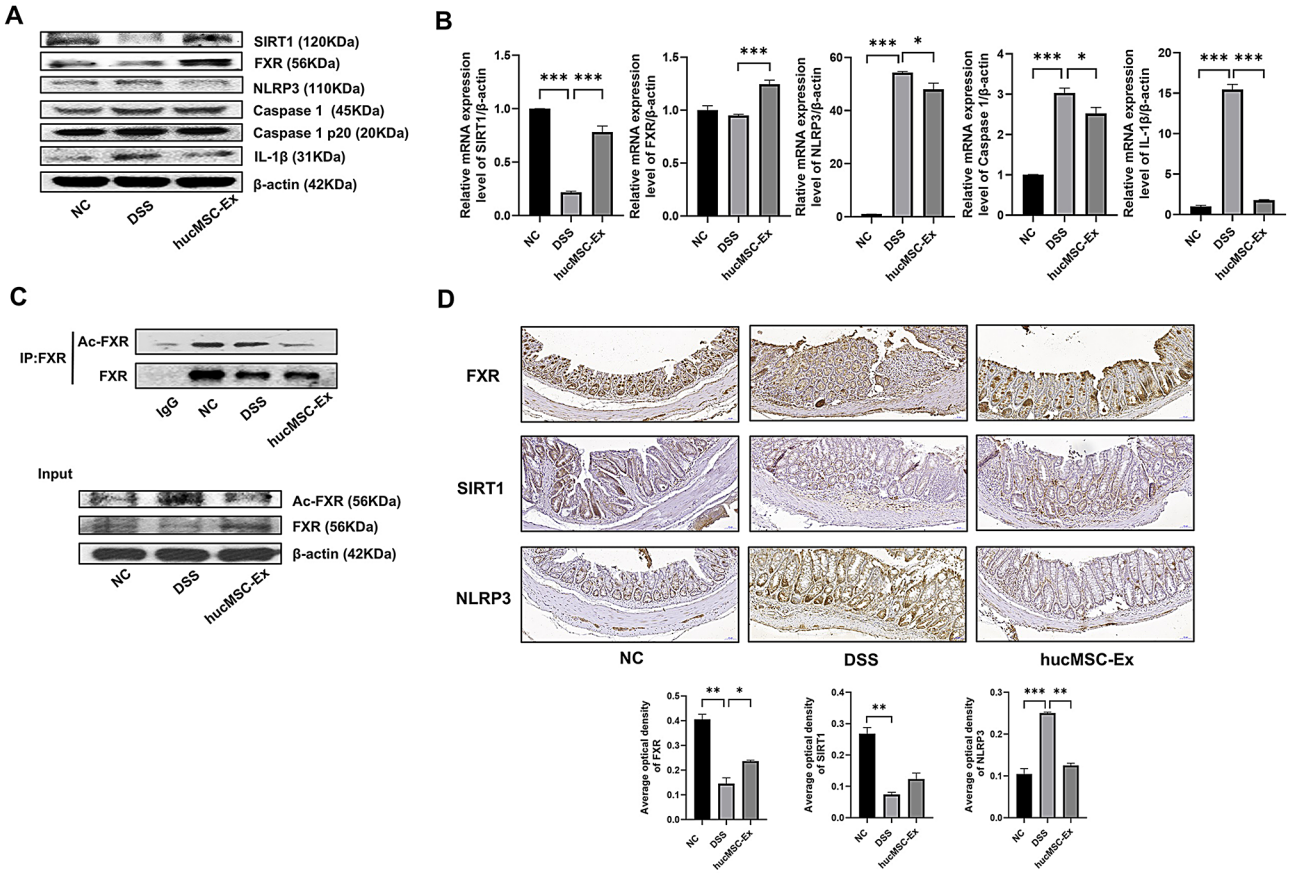

Fig. 4 hucMSC-Ex promotes the expression of SIRT1 and FXR while inhibits FXR acetylation and NLRP3 inflammasomes in mice colons. (**A)** The protein expression levels of SIRT1, FXR, and NLRP3 inflammasome-related molecules (NLRP3, Caspase 1, Caspase 1 p20, and IL-1β) in mice colon tissues by Western blot. (**B)** mRNA expression levels of SIRT1, FXR, and NLRP3 inflammasome-related molecules (NLRP3, Caspase 1, and IL-1β) in mice colon tissues by qRT-PCR; (**C)** The acetylation level of FXR in mouse colon tissues by IP test; **(D)** Expression of FXR, SIRT1, and NLRP3 in colon tissue by IHC (200×, scale bar = 50 μm) and the relevant average optical density analysis ($n = 3$ independent experiments). $^{*}P < 0.05$, $^{**}P < 0.01$, $^{***}P < 0.001$

Regarding the trend in the percentage of weight loss, the DSS + EX 527 group had more obvious deterioration after intraperitoneal injection of EX 527 compared to the DSS group. After hucMSC-Ex treatment, the weight loss was mitigated in the hucMSC-Ex + EX 527 group compared to the DSS + EX 527 group (Fig. 6A). The DAI score was higher in the DSS + EX527 group than all other groups. Tail vein administration of hucMSC-Ex alleviated the changes induced by the combination of EX 527 and DSS in mice, including loose stools, bloody stools, and weight loss (Fig. 6B). The hucMSC-Ex treatment mitigated colonic length shortening and splenomegaly in the hucMSC-Ex + EX 527 group relative to the DSS + EX 527 group (Fig. 6C, D). H&E staining of colon tissues of mice showed that the glandular structure in the DSS + EX 527 group was blurred compared to the DSS group, while that of the hucMSC-Ex + EX 527 group was clearer than the DSS + EX 527 group. After the intraperitoneal injection of EX527, the colon epithelial cells of IBD mice were damaged more seriously, the crypt structure was difficult to distinguish, and the inflammatory cell invasion was intensified. hucMSC-Ex could effectively alleviate the damage of EX527 to the colons (Fig. 6E). The splenic nodule structure of the DSS + EX 527 group was significantly damaged compared to the DSS group, with the hucMSC-Ex + EX 527 group exhibiting significantly intact nodular structure than the DSS + EX 527 group (Fig. 6F). The mRNA expression in the colon tissues by qRT-PCR indicated that pro-inflammatory factors TNF-α and IL-6 were upregulated in the DSS + EX 527 group compared to the hucMSC-Ex + EX 527 group. On the other hand, the anti-inflammatory factor IL-10 was downregulated in the DSS + EX 527 group compared to the hucMSC-Ex + EX 527 group (Fig. 6G). These data indicate that hucMSC-Ex significantly alleviates the inflammatory effects of EX 527 on IBD mice.

hucMSC-Ex inhibits FXR acetylation and NLRP3 inflammasomes by activating the SIRT1-FXR pathway in mice colon

The protein expression levels of SIRT1, FXR, and NLRP3 inflammasome-related molecules (NLRP3, Caspase 1,

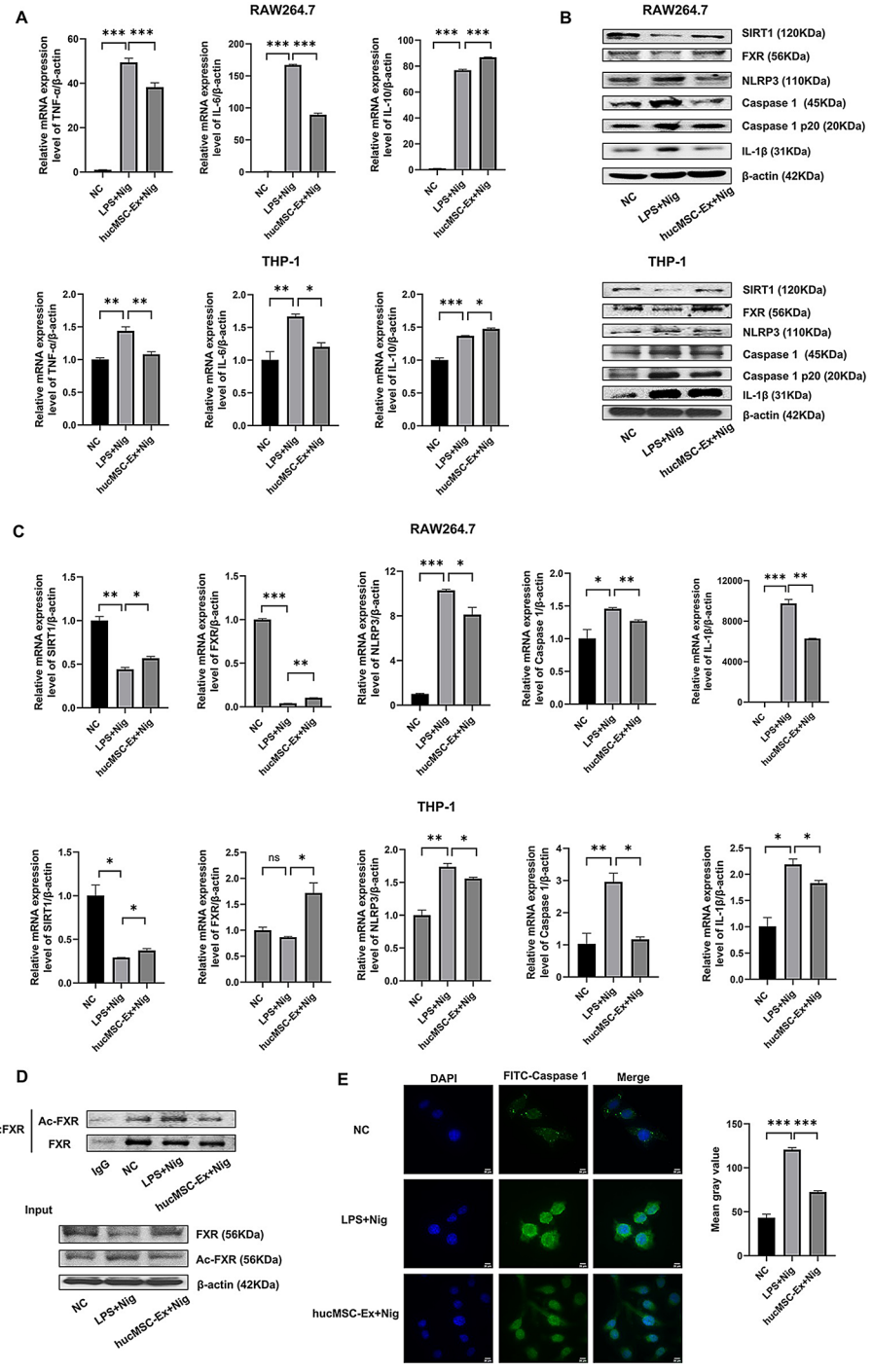

Fig. 5 hucMSC-Ex promotes the expression of SIRT1 and FXR, inhibiting FXR acetylation and NLRP3 inflammasomes in macrophages.**(A)** mRNA expression levels of inflammatory cytokines (TNF-α、IL-6, and IL-10) in RAW264.7 and THP-1 by qRT-PCR; (**B)** Western blot analysis of SIRT1, FXR, and NLRP3 inflammasome-related molecules (NLRP3, Caspase1, Caspase1 p20 and IL-1β) in RAW264.7 and THP-1; (**C)** mRNA expression levels of SIRT1, FXR, and NLRP3 inflammasome-related molecules (NLRP3, Caspase 1, and IL-1β) in RAW264.7 and THP-1 by qRT-PCR; (**D)** The acetylation level of FXR in RAW264.7 by IP; **(E)** The expression of Caspase 1 in RAW264.7 by IF and the mean gray value analysis of the IF of Caspase 1. $^{*}P < 0.05$, $^{**}P < 0.01$, $^{***}P < 0.001$

Caspase 1 p20, and IL-1β) in mice colon tissues were detected by Western blot. It was found that SIRT1 and FXR in the DSS + EX 527 group were lower than the DSS group, while NLRP3 inflammasome-related molecules were higher in the DSS + EX 527 group than the DSS group. After hucMSC-Ex treatment, SIRT1 and FXR increased while NLRP3 inflammasome-related molecules decreased in the hucMSC-Ex + EX 527

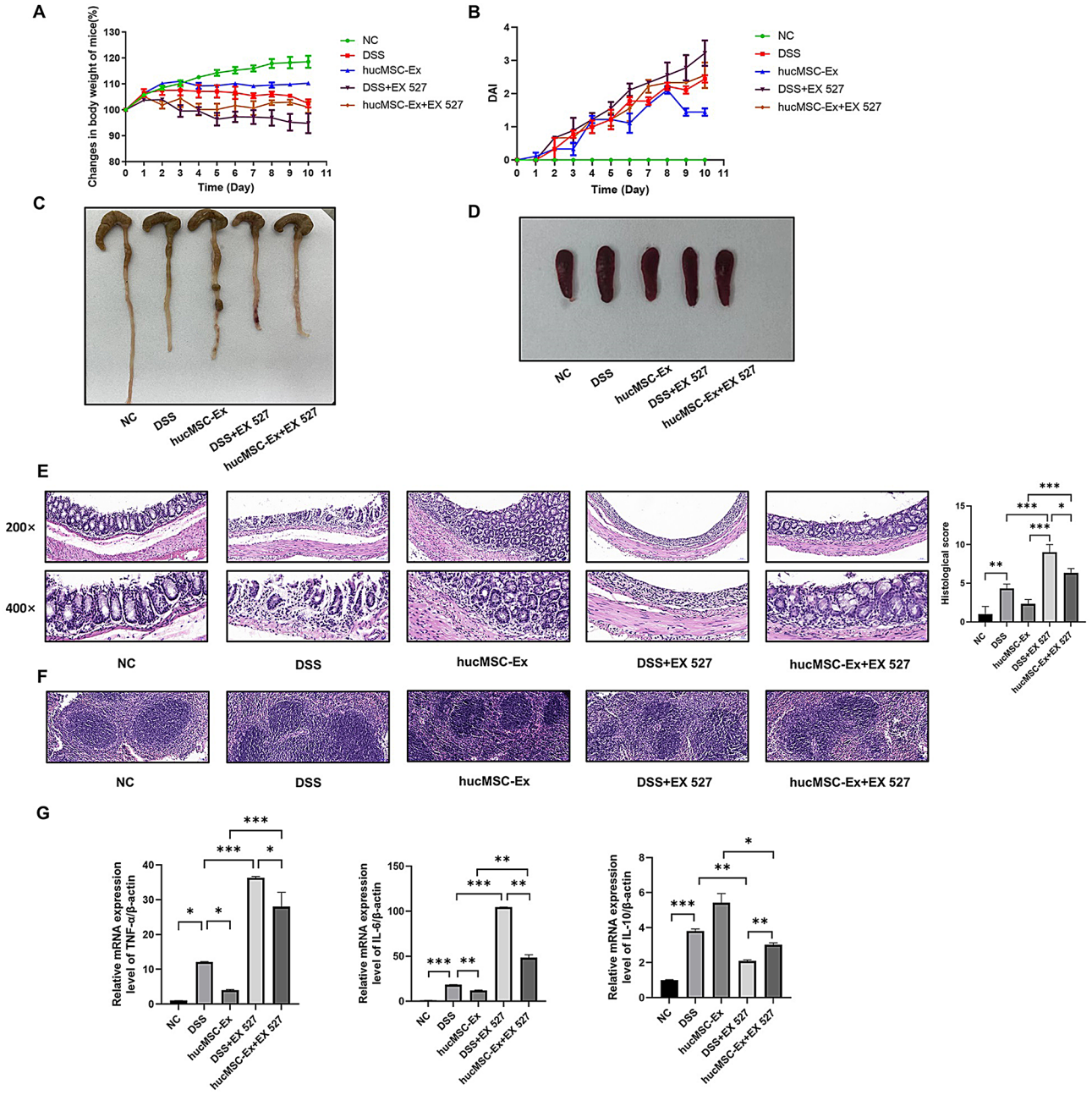

Fig. 6 hucMSC-Ex alleviates the effect of EX527 on IBD mice model. **(A)** Percentage of weight loss in mice ($n = 3$ independent experiments).; **(B)** Assessment of DAI in mice ($n = 3$ independent experiments); **(C)** Gross view of the colons of mice; **(D)** Gross view of the spleens of mice; **(E)** H&E staining of the colons of mice (200×, scale bar = 50 μm; 400×, scale bar = 20 μm) and the histological score of the colons of mice; **(F)** H&E staining of spleens of mice (200×, scale bar = 50 μm); **(G)** mRNA expression levels of inflammatory factors (TNF-α, IL-6 and IL-10) in colon tissues of mice by qRT-PCR ($n = 3$ independent experiments), $^{*}P < 0.05$, $^{**}P < 0.01$, $^{***}P < 0.001$

group compared to the DSS + EX 527 group (Fig. 7A). IP analysis showed that the FXR acetylation level in the DSS + EX 527 group was higher than the hucMSC-Ex + EX 527 group (Fig. 7B). Moreover, qRT-PCR showed a similar trend of reduced mRNA expression levels of SIRT1 and FXR in the colon of the DSS + EX 527 group compared to the hucMSC-Ex + EX 527 group, while NLRP3 inflammasome-related molecules were higher in the DSS + EX 527 group than the hucMSC-Ex + EX 527 group (Fig. 7C). IHC was employed to confirm these observations, with results showing reduced expression of SIRT1 and FXR but elevated NLRP3 in the DSS + EX 527 group and a reverse effect after hucMSC-Ex treatment (Fig. 7D).

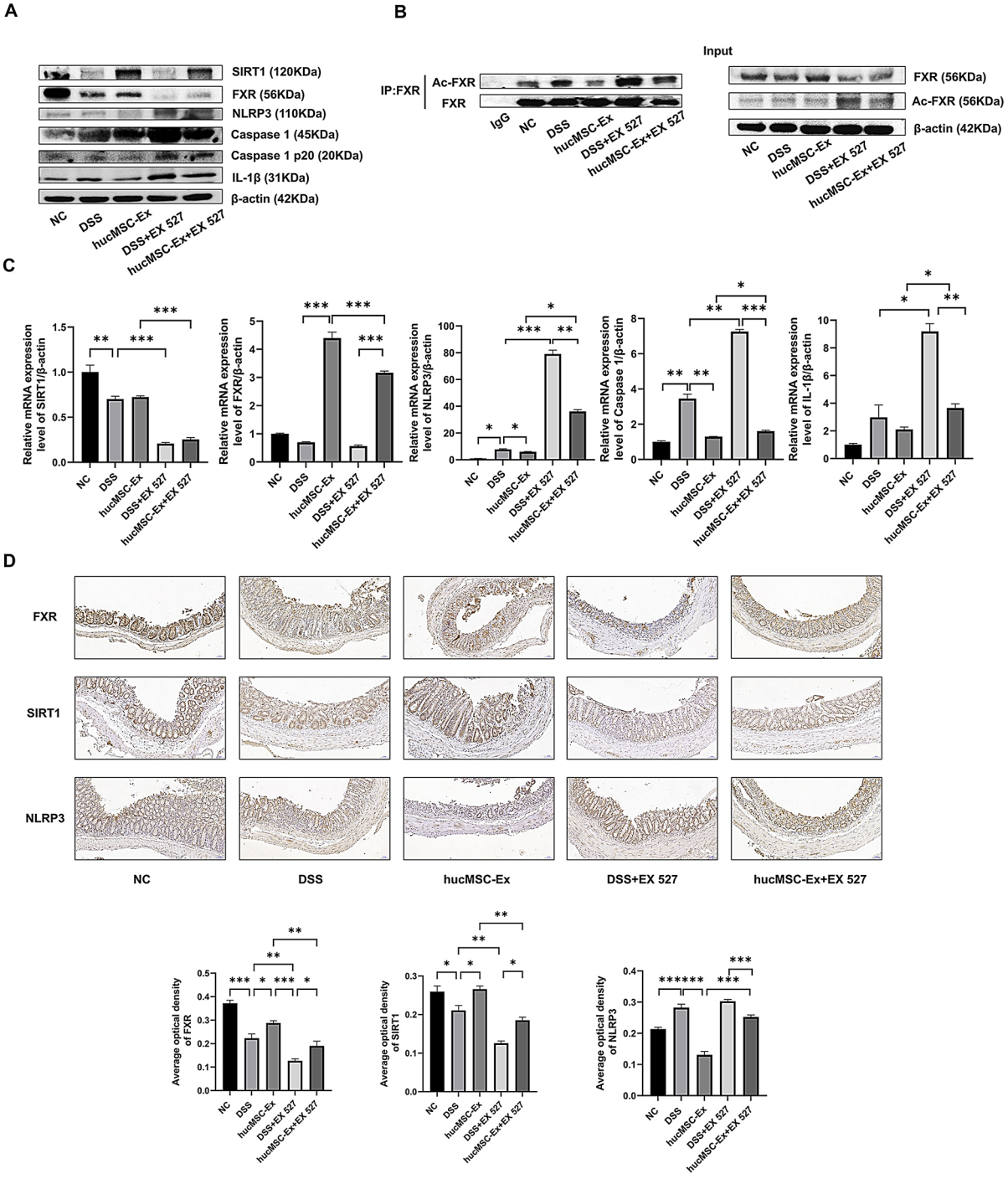

Fig. 7 hucMSC-Ex inhibits FXR acetylation by activating SIRT1-FXR pathway in mouse colon, directly hindering NLRP3 inflammasomes activation. (**A)** The protein expression levels of SIRT1, FXR, and NLRP3 inflammasome-related molecules (NLRP3, Caspase1, Caspase1 p20 and IL-1β) in mice colon tissues by Western blot. (**B)** The acetylation level of FXR in the colon tissues of mice by IP; (**C)** mRNA expression levels of SIRT1, FXR, and NLRP3 inflammasome-related molecules (NLRP3, Caspase 1 and IL-1β) in mice colon tissues by qRT-PCR; (**D)** Localization of FXR, SIRT1, and NLRP3 in colon tissues by IHC detection (200×, scale bar = 50 μm) and the relevant average optical density analysis ($n = 3$ independent experiments). *$P < 0.05$, **$P < 0.01$, ***$P < 0.001$

hucMSC-Ex inhibits FXR acetylation and NLRP3 inflammasomes by activating the SIRT1-FXR pathway in macrophages

The inflammatory factors TNF-α, IL-6, and IL-10 in RAW264.7 and THP-1 were assessed by qRT-PCR. Results indicated that pro-inflammatory factors TNF-α and IL-6 were upregulated and the anti-inflammatory factor IL-10 was downregulated in the LPS + EX

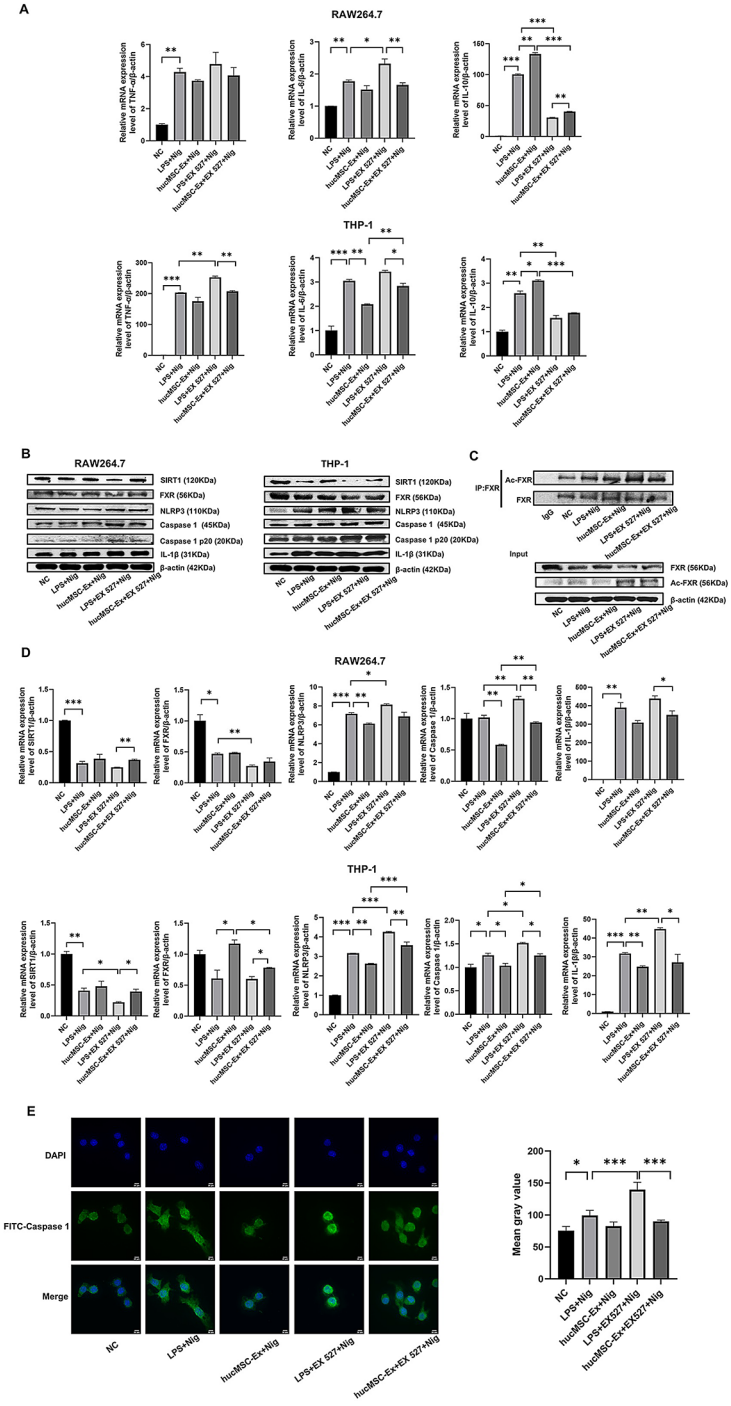

Fig. 8 hucMSC-Ex inhibits FXR acetylation by activating SIRT1-FXR pathway in macrophages, directly hindering NLRP3 inflammasomes activation. **(A)** mRNA expression levels of inflammatory factors (TNF-α, IL-6, and IL-10) in RAW264.7 and THP-1 by qRT-PCR; **(B)** Western blot analysis of the protein expression of SIRT1, FXR, and NLRP3 inflammasome-related molecules (NLRP3, Caspase 1, Caspase 1 p20, and IL-1β) in RAW264.7 and THP-1; (**C**)The acetylation level of FXR in RAW264.7 by IP; (**D**) mRNA expression levels of SIRT1, FXR, and NLRP3 inflammasome-related molecules (NLRP3, Caspase 1 and IL-1β) in RAW264.7 and THP-1 by qRT-PCR; **(E)** The expression of Caspase 1 in RAW264.7 by IF and the mean gray value analysis of the IF of Caspase 1.*$P < 0.05$, **$P < 0.01$, ***$P < 0.001$

527 + Nig group compared to the hucMSC-Ex + EX 527 + Nig group (Fig. 8A), implying that hucMSC-Ex alleviates the inflammatory effects of SIRT1 inhibitor EX 527 on macrophages. Western blot results showed a consistent trend with the qRT-PCR results, where the protein expression levels of SIRT1 and FXR were reduced and NLRP3 inflammasome-related molecules increased in the LPS + EX 527 + Nig group but reversed in effect in

the hucMSC-Ex + EX 527 + Nig group of RAW264.7 and THP-1 cells (Fig. 8B). IP results showed increased FXR acetylation level of RAW264.7 in the LPS + EX 527 + Nig group relative to the hucMSC-Ex + EX 527 + Nig group (Fig. 8C). qRT-PCR results confirmed a similar trend with Western blot results in SIRT1, FXR, and NLRP3 inflammasome expression in the LPS + EX 527 + Nig group and the hucMSC-Ex + EX 527 + Nig group (Fig. 8D), indicating the promoting effect of hucMSC-Ex on SIRT1 and FXR while downregulating NLRP3 inflammasome. IF analysis also showed the inhibition effect of hucMSC-Ex on Caspase 1, an NLRP3 inflammasome-related molecule (Fig. 8E).

Discussion

DSS-induced IBD mice are a chemically induced model of intestinal inflammation that appears similar to intestinal epithelial damage in human colitis. Typical histological changes in the acute model induced by DSS include depletion of mucin and goblet cells in the colon, erosion of the intestinal epithelium, ulceration, and granulocyte infiltration into the lamina and submucosa, leading to a violent inflammatory response [24].Adding DSS to drinking water can induce acute enteritis in mice, which can exhibit weight loss, loose stools, and bloody stools [25]. The IBD mouse model constructed in this study exhibited these characteristics, making them suitable for the study.

Exosomes of different origin have specific surface markers for identification, such as CD9, CD81, CD63, Alix, and HSP70. Exosomes contain a variety of bioactive components such as RNA (miRNA, lncRNA, and circRNA) and proteins [26]. In recent years, exosomes have been regarded as the basic mode of intercellular communication, and are widely involved in the regulation of cell proliferation, differentiation, and apoptosis. A large number of preclinical studies have shown that exosomes have important research value for disease treatment, including IBD [27].For example, hucMSC-Ex alleviates IBD by targeting long-chain acyl-CoA synthetase 4 (ACSL4) with its bioactive ingredient miR-129-5p to inhibit lipid peroxidation and iron death, while inhibiting intestinal inflammatory responses and blocking apoptosis [28]. Because of its high content, easy access, and stable structure, it can be used as a biomarker for early disease diagnosis and monitoring [29]. At present, hucMSC-Ex has been reported to relieve liver fibrosis, diabetes, kidney damage, and other diseases [30–32]. Our data indicates that the injection of hucMSC-Ex through the tail vein can effectively alleviate the weight loss, loose stool, bloody stool, and mental state of mice relative to the untreated DSS group. Compared to the DSS group, mice in the hucMSC-Ex group had longer colons length, reduced spleen enlargement, restored colonic and splenic tissue structure, increased anti-inflammation, and reduced pro-inflammatory factors. This suggests that hucMSC-Ex can repair DSS-induced IBD in mice.

FXR is an important safeguard for intestinal health. In the IBD model, selective activation of FXR in the gut can play a protective role, and FXR is also a regulator of intestinal lymphocytes [33]. Some studies have found that the mechanism by which FXR agonist GW4064 effectively alleviates IBD lies in its activation of FXR expression, regulating intestinal barrier function and playing a key role in coordinating inflammation and mitochondrial dysfunction [34].Since the expression of FXR in the colon tissues of healthy people is higher than IBD patients, and Ac-Lys is lower in healthy people than IBD patients, we speculated that the pathogenesis of IBD may be related to the acetylation level of FXR, while SIRT1 is related to the acetylation level of FXR, and FXR can contribute to the inhibition of the activity of NLRP3 inflammasomes. To clarify the correlation, an animal model of IBD was established using mice. It was found that the mRNA and protein expression levels of SIRT1 and FXR were decreased while the acetylation of FXR and the expression of NLRP3 inflammation -related molecules were increased in the colon tissues of mice under the effect of DSS. These data indicate that the progression of IBD was related to the acetylation level of FXR. Compared to the DSS group, hucMSC-Ex promoted the expression of SIRT1 and FXR in the colon tissues of mice, and the acetylation level of FXR in the hucMSC-Ex group was lower than that of the DSS group. Meanwhile, hucMSC-Ex also inhibited the activation of NLRP3 inflammasome in the colon of mice. This implies that hucMSC-Ex can regulate the acetylation level of FXR and inhibit the activation of NLRP3 inflammasome in the process of repairing IBD.

An earlier study reported that the SIRT1-FXR pathway plays an important role in liver diseases, and by activating this pathway, glucoside can alleviate liver fibrosis induced by biliary ligation and promote the expression of SIRT1. FXR was subsequently deacetylated and the bile acid profile was restored, effectively protecting the liver [35].Melatonin regulates bile acid metabolism by activating the SIRT1-FXR signaling axis, effectively alleviates necrotizing enterocolitis, and reverses the abnormal expression of bile acid transport-related proteins [36].However, this pathway has been poorly studied in the pathogenesis of IBD. EX 527 has been widely used to inhibit SIRT1 expression in animal models, including in the mouse model of IBD, with certain safety and applicability, and can play a rapid and efficient role in inhibiting SIRT1 expression in the colon of mice [37, 38].After the intraperitoneal injection of SIRT1 inhibitor EX 527, the IBD mice experienced severe weight loss, increased degree of loose and bloody stool, worsened mental state, obvious destruction of colon and spleen tissue structure,

and serious inflammatory reaction, which accelerated the development of IBD. The administration of hucMSC-Ex's via tail vein alleviated the influence of EX 527 on IBD mice. The results of Western blot, qRT-PCR, IP, and IHC showed that the expression of SIRT1 and FXR in the colon of mice were simultaneously inhibited under the influence of EX 527, and the acetylation level of FXR was increased. However, the injection of hucMSC-Ex in the tail vein alleviated the influence of EX 527. Therefore, hucMSC-Ex can activate the SIRT1-FXR pathway in the colon of IBD mice and reduce FXR acetylation level. At the same time, the increase of FXR acetylation level caused by EX 527 was accompanied by the enhancement of the activity of NLRP3 inflammasome. After hucMSC-Ex tail vein injection, the acetylation level of FXR decreased and the activity of NLRP3 inflammasome was also inhibited, indicating that the acetylation level of FXR was positively correlated with the activity of NLRP3 inflammasome in the colon of mice.

Since the pathogenesis of IBD is related to immune disorders, intestinal homeostasis is jointly regulated by epithelial cells and immune cells, and studies have found that the sensing of abnormal bile acid levels by internal FXR of intestinal macrophages leads to the secretion of pro-inflammatory cytokines and the subsequent promotion of the proliferation of intestinal stem cells [22]. Activation of FXR can regulate the recruitment and polarization of intestinal macrophages and crosstalk with Th17 cells to alleviate intestinal inflammation and inhibit the growth of related tumors. Thus, the regulatory effect of FXR on intestinal macrophages may be an effective target for IBD treatment [22].The presence of macrophages is one of the necessary conditions for wound healing, and the insufficient expression of SIRT1 in macrophages can promote oxidative stress and activate inflammatory pathways, hinder wound healing, and accelerate scar hyperplasia [39].Therefore, changes in the expression of SIRT1 and FXR in macrophages can affect the function of macrophages. At the same time, the activation of NLRP3 inflammasome is also an important part of the proinflammatory function of macrophages [40], Our results showed that hucMSC-Ex could increase the mRNA and protein expression levels of SIRT1 and FXR in macrophages, and decrease NLRP3 inflammasome-related molecules. The level of FXR acetylation in macrophages in the hucMSC-Ex + Nig group was lower than the LPS + Nig group. Thus, hucMSC-Ex not only promoted the expression of SIRT1 and FXR but also downregulated the acetylation modification of FXR. Therefore, we successfully demonstrated that hucMSC-Ex can promote the expression of SIRT1 and FXR in macrophages, inhibit the level of FXR acetylation, and negatively regulate the activation of NLRP3 inflammasomes, which reveals a new mechanism in the hucMSC-Ex repair of IBD.

The addition of EX 527 further promoted the expression of pro-inflammatory factors in the macrophage inflammatory model, while hucMSC-Ex alleviated the inflammatory effects of EX 527. Meanwhile, EX 527 further decreased the expression of SIRT1 and FXR in macrophages, resulting in a higher acetylation level of FXR. The expression of NLRP3 inflammasome related molecules was further increased, indicating that the FXR acetylation level of macrophages was related to the activity of NLRP3 inflammasome. The addition of hucMSC-Ex reduced the effect of EX 527. It was confirmed that hucMSC-Ex could inhibit the activation of NLRP3 inflammasomes by activating the SIRT1-FXR pathway in macrophages, thereby reducing the level of FXR acetylation.

This study provides a new mechanism for hucMSC-Ex to repair IBD and lays a foundation for future hucMSC-Ex research. However, there are still some deficiencies in our research. Since hucMSC-Ex contains many bioactive ingredients, the specific key biomolecule(s) that play(s) a role in activating the SIRT1-FXR pathway is yet to be established. Moreover, macrophages have M1 and M2 types. Whether hucMSC-Ex activation of the SIRT1-FXR pathway is accompanied by macrophage polarization has not been studied. In addition, FXR is a key receptor that regulates bile acid metabolism, and whether the hucMSC-Ex activation of the SIRT1-FXR pathway to repair IBD is accompanied by changes in bile acid levels is yet to be studied. Therefore, more studies are worth further exploring the repair effect of hucMSC-Ex via the regulation of FXR in IBD.

Conclusion

HucMSC-Ex reduces the acetylation level of FXR by activating the SIRT1-FXR pathway in macrophages, and negatively regulates the activation of NLRP3 inflammasomes, inhibiting the occurrence of the inflammatory response and alleviating IBD. The discovery of hucMSC-Ex, a "new activator" of FXR, may reduce side effects of current activators and presents promising clinical application value and prospects in IBD.

Abbreviations

IBD	Inflammatory Bowel Disease
hucMSC-Ex	Human Umbilical Cord Mesenchymal Stem Cell-Derived Exosomes
MVB	Multivesicular Body
LPS	Lipopolysaccharide
Nig	Nigericin
FXR	Farnesoid X receptor
SIRT1	Silent Information Regulator of Transcription 1
TNF-α	Tumor Necrosis Factor-α
TMIGD1	Transmembrane and Immunoglobulin Domain Containing 1
MCP-1	Monocyte Chemotactic Protein-1
CDCA	Chenodeoxycholic Acid
NAFLD	Nonalcoholic Fatty Liver Disease
IP	Immunoprecipitation
IHC	Immunohistochemistry

IF	Immunofluorescence
DSS	Dextran Sulfate Sodium Salt
NLRP3	NOD-Like Receptor Thermal Protein Domain Associated Protein 3
Ac-Lys	Acetylated-Lysine
Caspase 1	Cysteinyl Aspartate Specific Proteinase 1
HSP70	Heat Shock Protein 70
ACSL4	Long-Chain Acyl-CoA Synthetase 4

Supplementary Information

The online version contains supplementary material available at https://doi.org/10.1186/s13287-025-04365-8.

Supplementary Material 1

Supplementary Material 2

Acknowledgements
The authors declare that they have not use AI-generated work in this manuscript.

Author contributions
Mengjiao Zhou: conception and design, collection and/or assembly of data, data analysis and interpretation, and manuscript writing. Bing Pei: collection and assembly of data, data analysis and interpretation, and manuscript writing. Peipei Cai: data interpretation. Chengxue Yi: data analysis and interpretation. Francis Atim Akanyibah and Changkun Lyu: collection and/or assembly of data and interpretation. Fei Mao: study design, data analysis and interpretation, and final approval of manuscript. All authors read and approved the final manuscript.

Funding
Zhenjiang key research and development plan (social development) (Grant no. SH2023050), Jiangsu Province Six Talents Project (YY-230), henan province 2024 science and technology development plan (Grant No. 242102310081), the open topic at the university level of Shangqiu Medical College in 2023 (Grant No. KFKT23005) and Jiangsu Provincial Medical Key Discipline Cultivation Unit (Grant No. JSDW202241).

Data availability
All data and materials generated and analyzed during this study are available from the corresponding author on reasonable request. All additional files are included in the manuscript.

Declarations

Ethics approval and consent to participate
The ethics of animal research was approved by the Ethical Committee of Jiangsu University. [Approval title: Study on the role and mechanism of exosomes derived from hucMSC in regulating Neddylation in the repair of inflammatory bowel disease.] [Approval number: 2012258] (Approval date: 2020.3.31). The ethics of the human specimens in this study was approved by the Ethics Committee of Zhenjiang First People's Hospital. [Approval title: Study on the Mechanism of HucMSC-Ex regulating FXR Expression to inhibit Ferroptosis in Repairing IBD.] [Approval number: SQK-20240196-Y] (Approval date: 2024.9.27). And the Original Source (Procell) of THP-1 cells has confirmed initial ethical approval for the collection of human cells, and the donor has signed an informed consent form.

Consent for publication
Not applicable.

Competing interests
The authors declare that they have no competing interests.

Received: 26 October 2024 / Accepted: 24 April 2025
Published online: 09 May 2025

References

1. Qiu P, Ishimoto T, Fu L, Zhang J, Zhang Z, Liu Y. The gut microbiota in inflammatory bowel disease. Front Cell Infect Microbiol. 2022;12:733992. https://doi.org/10.3389/fcimb.2022.
2. Dowdell AS, Colgan SP. Metabolic Host-Microbiota interactions in autophagy and the pathogenesis of inflammatory bowel disease (IBD). Pharmaceuticals (Basel). 2021;14(8). https://doi.org/10.3390/ph14080708.
3. Uranga JA, López-Miranda V, Lombó F, Abalo R. Food, nutrients and nutraceuticals affecting the course of inflammatory bowel disease. Pharmacol Rep. 2016;68(4):816–26. https://doi.org/10.1016/j.pharep.2016.05.002.
4. Ghouri YA, Tahan V, Shen B. Secondary causes of inflammatory bowel diseases. World J Gastroenterol. 2020;26(28):3998–4017. https://doi.org/10.3748/wjg.v26.i28.3998.
5. Lai P, Weng J, Guo L, Chen X, Du X. Novel insights into MSC-EVs therapy for immune diseases. Biomark Res. 2019;7:6. https://doi.org/10.1186/s40364-019-0156-0.
6. Zhang L, Yu D. Exosomes in cancer development, metastasis, and immunity. Biochim Biophys Acta Rev Cancer. 2019;1871(2):455–68. https://doi.org/10.1016/j.bbcan.2019.04.004.
7. Hade MD, Suire CN, Suo Z. Mesenchymal stem Cell-Derived exosomes: applications in regenerative medicine. Cells. 2021;10(8). https://doi.org/10.3390/cells10081959.
8. Chang X, Song Y-H, Xia T, He Z-X, Zhao S-B, Wang Z-J, et al. Macrophage-derived exosomes promote intestinal mucosal barrier dysfunction in inflammatory bowel disease by regulating TMIGD1 via mircroRNA-223. Int Immunopharmacol. 2023;121:110447. https://doi.org/10.1016/j.intimp.2023.110447.
9. Yu H, Yang X, Xiao X, Xu M, Yang Y, Xue C, Li X, Wang S, Zhao RC. Human adipose mesenchymal stem Cell-derived exosomes protect mice from DSS-Induced inflammatory bowel disease by promoting Intestinal-stem-cell and epithelial regeneration. Aging Dis. 2021;12(6):1423–37. https://doi.org/10.14336/AD.2021.0601.
10. Jiang L, Zhang H, Xiao D, Wei H, Chen Y. Farnesoid X receptor (FXR): structures and ligands. Comput Struct Biotechnol J. 2021;19:2148–59. https://doi.org/10.1016/j.csbj.2021.04.029.
11. Kemper JK, Xiao Z, Ponugoti B, Miao J, Fang S, Kanamaluru D, et al. FXR acetylation is normally dynamically regulated by p300 and SIRT1 but constitutively elevated in metabolic disease States. Cell Metab. 2009;10(5):392–404. https://doi.org/10.1016/j.cmet.2009.09.009.
12. Zhao Q, Liu F, Cheng Y, Xiao X-R, Hu D-D, Tang Y-M, et al. Celastrol protects from cholestatic liver injury through modulation of SIRT1-FXR signaling. Mol Cell Proteom. 2019;18(3):520–33. https://doi.org/10.1074/mcp.RA118.000817.
13. Yang J, Sun L, Wang L, Hassan HM, Wang X, Hylemon PB, et al. Activation of Sirt1/FXR signaling pathway attenuates Triptolide-Induced hepatotoxicity in rats. Front Pharmacol. 2017;8:260. https://doi.org/10.3389/fphar.2017.00260.
14. Fiorucci S, Zampella A, Ricci P, Distrutti E, Biagioli M. Immunomodulatory functions of FXR. Mol Cell Endocrinol. 2022;551:111650. https://doi.org/10.1016/j.mce.2022.111650.
15. Yunna C, Mengru H, Lei W, Weidong C. Macrophage M1/M2 polarization. Eur J Pharmacol. 2020;877:173090. https://doi.org/10.1016/j.ejphar.2020.173090.
16. Li C, Xu MM, Wang K, Adler AJ, Vella AT, Zhou B. Macrophage polarization and meta-inflammation. Transl Res. 2018;191:29–44. https://doi.org/10.1016/j.trsl.2017.10.004.
17. Zhang K, Guo J, Yan W, Xu L. Macrophage polarization in inflammatory bowel disease. Cell Commun Signal. 2023;21(1):367. https://doi.org/10.1186/s12964-023-01386-9.
18. Na YR, Stakenborg M, Seok SH, Matteoli G. Macrophages in intestinal inflammation and resolution: a potential therapeutic target in IBD. Nat Rev Gastroenterol Hepatol. 2019;16(9):531–43. https://doi.org/10.1038/s41575-019-0172-4.
19. Olona A, Leishman S, Anand PK. The NLRP3 inflammasome: regulation by metabolic signals. Trends Immunol. 2022;43(12):978–89. https://doi.org/10.1016/j.it.2022.10.003.
20. Li L, Zhang Q, Peng J, Jiang C, Zhang Y, Shen L, Dong J, Wang Y, Jiang Y. Activation of farnesoid X receptor downregulates monocyte chemoattractant protein-1 in murine macrophage. Biochem Biophys Res Commun. 2015;467(4):841–6. https://doi.org/10.1016/j.bbrc.2015.
21. Yao J, Zhou C-S, Ma X, Fu B-Q, Tao L-S, Chen M, Xu Y-P. FXR agonist GW4064 alleviates endotoxin-induced hepatic inflammation by repressing macrophage activation. World J Gastroenterol. 2014;20(39):14430–41. https://doi.org/10.3748/wjg.v20.i39.14430.

22. Dong X, Qi M, Cai C, Zhu Y, Li Y, Coulter S, et al. Farnesoid X receptor mediates macrophage-intrinsic responses to suppress colitis-induced colon cancer progression. JCI Insight. 2024;9(2). https://doi.org/10.1172/jci.insight.170428.
23. Garcia-Irigoyen O, Moschetta A. A novel protective role for FXR against inflammasome activation and endotoxemia. Cell Metab. 2017;25(4):763–4. https://doi.org/10.1016/j.cmet.2017.03.014.
24. Eichele DD, Kharbanda KK. Dextran sodium sulfate colitis murine model: an indispensable tool for advancing our Understanding of inflammatory bowel diseases pathogenesis. World J Gastroenterol. 2017;23(33):6016–29. https://doi.org/10.3748/wjg.v23.i33.6016.
25. Kim JJ, Shajib MS, Manocha MM, Khan WI. Investigating intestinal inflammation in DSS-induced model of IBD. J Vis Exp. 2012(60). https://doi.org/10.3791/3678
26. Li S, Yi M, Dong B, Tan X, Luo S, Wu K. The role of exosomes in liquid biopsy for cancer diagnosis and prognosis prediction. Int J Cancer. 2021;148(11):2640–51. https://doi.org/10.1002/ijc.33386.
27. Dwivedi M, Ghosh D, Saha A, Hasan S, Jindal D, Yadav H, Yadava A, Dwivedi M. Biochemistry of exosomes and their theranostic potential in human diseases. Life Sci. 2023;315:121369. https://doi.org/10.1016/j.lfs.2023.121369.
28. Wei Z, Hang S, Wiredu Ocansey DK, Zhang Z, Wang B, Zhang X, Mao F. Human umbilical cord mesenchymal stem cells derived exosome shuttling mir-129-5p attenuates inflammatory bowel disease by inhibiting ferroptosis. J Nanobiotechnol. 2023;21(1):188. https://doi.org/10.1186/s12951-023-01951-x.
29. Zhang Q, Wang H, Liu Q, Zeng N, Fu G, Qiu Y, et al. Exosomes as powerful biomarkers in cancer: recent advances in isolation and detection techniques. Int J Nanomed. 2024;19:1923–49. https://doi.org/10.2147/IJN.S453545.
30. Li T, Yan Y, Wang B, Qian H, Zhang X, Shen L, et al. Exosomes derived from human umbilical cord mesenchymal stem cells alleviate liver fibrosis. Stem Cells Dev. 2013;22(6):845–54. https://doi.org/10.1089/scd.2012.0395.
31. Sun Y, Shi H, Yin S, Ji C, Zhang X, Zhang B, et al. Human mesenchymal stem cell derived exosomes alleviate type 2 diabetes mellitus by reversing peripheral insulin resistance and relieving β-Cell destruction. ACS Nano. 2018;12(8):7613–28. https://doi.org/10.1021/acsnano.7b07643.
32. Wan Y, Yu Y, Yu C, Luo J, Wen S, Shen L, Wei G, Hua Y. Human umbilical cord mesenchymal stem cell exosomes alleviate acute kidney injury by inhibiting pyroptosis in rats and NRK-52E cells. Ren Fail. 2023;45(1):2221138. https://doi.org/10.1080/0886022X.2023.2221138.
33. Fu T, Li Y, Oh TG, Cayabyab F, He N, Tang Q, et al. FXR mediates ILC-intrinsic responses to intestinal inflammation. Proc Natl Acad Sci U S A. 2022;119(51):e2213041119. https://doi.org/10.1073/pnas.2213041119.
34. Liu H-M, Liao J-F, Lee T-Y. Farnesoid X receptor agonist GW4064 ameliorates lipopolysaccharide-induced Ileocolitis through TLR4/MyD88 pathway related mitochondrial dysfunction in mice. Biochem Biophys Res Commun. 2017;490(3):841–8. https://doi.org/10.1016/j.bbrc.2017.06.129.
35. Qin T, Hasnat M, Wang Z, Hassan HM, Zhou Y, Yuan Z, Zhang W. Geniposide alleviated bile acid-associated NLRP3 inflammasome activation by regulating SIRT1/FXR signaling in bile duct ligation-induced liver fibrosis. Phytomedicine. 2023;118:154971. https://doi.org/10.1016/j.phymed.2023.
36. Lai J, Li F, Li H, Huang R, Ma F, Gu X, et al. Melatonin alleviates necrotizing Enterocolitis by reducing bile acid levels through the SIRT1/FXR signalling axis. Int Immunopharmacol. 2024;128:111360. https://doi.org/10.1016/j.intimp.2023.111360.
37. Wang S, Deng W, Li F, Xiang L, Lv P, Chen Y. Treatment with butyrate alleviates dextran sulfate sodium and Clostridium difficile-induced colitis by preventing activity of Th17 cells via regulation of SIRT1/mTOR in mice. J Nutr Biochem. 2023;111:109155. https://doi.org/10.1016/jjnutbio.2022.109155.
38. Akimova T, Xiao H, Liu Y, Bhatti TR, Jiao J, Eruslanov E, et al. Targeting sirtuin-1 alleviates experimental autoimmune colitis by induction of Foxp3 + T-regulatory cells. Mucosal Immunol. 2014;7(5):1209–20. https://doi.org/10.1038/mi.2014.10.
39. He T, Bai X, Li Y, Zhang D, Xu Z, Yang X, Hu D, Han J. Insufficient SIRT1 in macrophages promotes oxidative stress and inflammation during scarring. J Mol Med (Berl). 2023;101(11):1397–407. https://doi.org/10.1007/s00109-023-02364-x.
40. Zhang J, Liu X, Wan C, Liu Y, Wang Y, Meng C, Zhang Y, Jiang C. NLRP3 inflammasome mediates M1 macrophage polarization and IL-1β production in inflammatory root resorption. J Clin Periodontol. 2020;47(4):451–60. https://doi.org/10.1111/jcpe.13258.

Publisher's note